Transmembrane Domain V of the Endothelin-A Receptor Is a Binding Domain of ET_A-Selective TTA-386-Derived Photoprobes†

Sophie Tessier,‡ Stéphane Boivin,‡ Jacinthe Aubin,‡ Philipe Lampron,‡ Michel Detheux,§ and Alain Fournier*,‡

Institut National de la Recherche Scientifique−Institut Armand-Frappier, Université du Québec, 245 boulevard Hymus, Pointe-Claire (Montréal), Québec, Canada, H9R 1G6, and Euroscreen SA, 802 route de Lennik, 1070 Bruxelles, Belgique

Received January 15, 2005; Revised Manuscript Received March 24, 2005

ABSTRACT: On the basis of the structure of TTA-386, a specific antagonist of the endothelin-A receptor subtype (ET_A), photosensitive analogues were developed to investigate the binding domain of the receptor. Among those, a derivative containing, in position 6, the photoreactive amino acid D- or L-*p*-benzoyl-phenylalanine showed pharmacological properties very similar to those of TTA-386. Affinity of the probes were also evaluated on transfected CHO cells overexpressing the human ET_A receptor. Data showed that binding of the radiolabeled peptides were inhibited by ET-1 and BQ-610. Therefore, these photolabile probes were used to label the ET_A receptor found in CHO cells. Photolabeling produced a ligand−protein complex appearing on SDS−PAGE at around 66 kDa. An excess of ET-1 or BQ-610 completely abolished the formation of the complex showing the selectivity of the photoprobes. Digestions of the [^{125}I-Tyr^5, D- or L-Bpa^6]TTA-386−ET_A complex were carried out, and receptor fragments were analyzed to define the region of the receptor where the ligand interacted. Results showed that Endo Lys-C digestion gave a 4.8 kDa fragment corresponding to the Asp^{256}−Lys^{299} segment, whereas migration after V8 digestion revealed a fragment of 2.9 kDa. Because the fragments of these two digestions must overlap, the latter would be the Trp^{257}−Glu^{281} stretch. A cleavage with CNBr confirmed the identity of the binding domain by giving a fragment of 3.9 kDa corresponding to Glu^{249}−Met^{278}. Thus, the combined cleavage data strongly suggested that the binding domain of ET_A includes a portion of the fifth transmembrane domain, between residues Trp^{257} and Met^{278}.

Endothelin (ET)[1] is a polypeptide that was first isolated from the culture medium of porcine aortic endothelial cells (*1*). This hormone is primarily involved in the regulation of the cardiovascular system where it acts as one of the most potent vasoconstrictors known. Moreover, ET is also implicated in other biological activities, such as neurotransmission and modulation of cell processes including calcium transport, mitosis, and expression of many genes (*2*).

Analysis of the ET gene revealed the existence of three distinct isoforms named ET-1, ET-2, and ET-3 (*3*). All those peptides include 21 residues and exhibit important sequence similarities. In particular, they all contain two intramolecular disulfide bonds in positions 1−15 and 3−11. Effects of ET are mediated via two different receptors designated as ET_A and ET_B (*4*). These two subtypes of receptor were cloned and pharmacologically characterized (*5*). The ET receptors belong to the seven transmembrane G-protein coupled receptor superfamily, and their similarity at the amino acid level is at around 68%. Activation of the ET_A receptors found on vascular smooth muscle cells generates a sustained vasoconstriction. On the other hand, the vascular ET_B receptors are mostly localized on endothelial cells, and they mediate a vasodilatation through the release of nitric oxide. However, a subtype of ET_B receptor is located on the vascular smooth muscle cells where it also partly mediates their constriction (*6*). Hence, malfunctions of the ET system could be involved in diseases such as hypertension, local ischaemia including myocardial infarction, and renal and heart failure (*7*−*10*).

The classification of ET receptors was initially established on the different activity and binding profiles obtained with the ET peptide isoforms. To date, a few studies have been carried out to elucidate which segments of the ET receptors are crucial for ligand selectivity, activity, and affinity (*11*). For instance, site-directed mutagenesis showed that a large number of amino acids within ET_A, such as Gly^{97}, Lys^{140}, Lys^{159}, Gln^{165}, and Phe^{315}, located in transmembrane (TM) regions 1, 2, 3, 3, and 6, respectively, influence ET-1 binding

† Financial support was obtained from the Canadian Institutes for Health Research (CIHR). A.F. is "Chercheur National" from the Fonds de la Recherche en Santé du Québec (FRSQ). S.T. receives a studentship from the Heart and Stroke Foundation of Canada (HSFC). S.B. and P.L. are recipients of a studentship from the Natural Sciences and Engineering Research Council of Canada (NSERC).

* To whom correspondence should be addressed. Tel: (514) 630-8816. Fax: (514) 630-8850. E-mail: alain.fournier@iaf.inrs.ca.

‡ Université du Québec.

§ Euroscreen SA.

[1] Abbreviations: ACN, acetonitrile; Aebsf, 4-(2-aminoethyl)-benzene-sulfonyl fluoride; Boc, *tert*-butyloxycarbonyl; BOP, benzotriazol-1-yl-oxy-tris(dimethylamino)phosphonium hexafluorophosphate; Bpa, *p*-benzoyl-phenylalanine; BSA, bovine serum albumine; CHO cells, Chinese hamster ovary cells; CNBr, cyanogen bromide; DIPEA, diisopropylethylamine; DMF, dimethylformamide; ECL, enhanced chemiluminescence; equiv, equivalent; ET, endothelin; ET_A and ET_B, endothelin type A and type B receptors, respectively; GPCR, G protein-coupled receptor; HF, hydrogen fluoride; MALDI-TOF, matrix-assisted laser desorption ionisation-time-of-flight; PAGE, polyacrylamide gel electrophoresis; PVDF, polyvinylidene fluoride; SDS, sodium dodecyl sulfate; SEM, standard error of the mean; Suc, succinoyl; TFA, trifluoroacetic acid; TM, transmembrane.

10.1021/bi0500933 CCC: $30.25
Published on Web 04/28/2005

(*12*). In addition, molecular modeling and site-directed mutagenesis studies identified a few nonconserved amino acids in ET_A and ET_B receptors that could be implicated in ligand selectivity. For instance, it was concluded that Tyr^{129} (*13*, *14*) and Lys^{140} (*15*), in the second TM domain of ET_A receptors, and Lys^{181}, in the third TM domain of ET_B receptors, play a crucial role in the ET binding (*16*). It was also suggested that the ET receptors could be divided into two distinct parts, yet TM domains I, II, III, and VII would be involved in the ligand selectivity, while TM domains IV, V, and VI would be responsible for the binding process (*17*). So far, chimeric ET_A and ET_B receptors have been produced for the elucidation of a specific domain that influences the affinity of the receptor toward BQ-123, a selective ET_A antagonist. Thus, substitution of the first extracellular loop domain of the ET_A receptor with the corresponding domain of the ET_B receptor reduced drastically the inhibition by BQ-123, while the replacements of other extracellular domains of ET_A did not. These observations suggested that the first extracellular loop domain of the ET_A receptor is involved in ligand binding (*18)*.

All these studies, mainly using site-directed mutagenesis, provided clues on some residues and their ability to modulate the ET_A receptor−ligand complex formation and activation. However, to further characterize the amino acids involved in these biological processes, other analytical methods had to be explored. We then focused on photoaffinity labeling followed by fragmentation of the resulting photoligand−receptor complex for identifying sites of interaction between the ligand and the receptor. Benzoyl-phenylalanine (Bpa) (*19*), a photosensitive amino acid employed successfully to probe the substance P receptor *(20*), angiotensin II receptor (*21*), and urotensin II receptor (GPR14) (*22*), was exploited as a photolabile moiety.

In this paper, we describe the development of photoreactive probes derived from TTA-386, an antagonist compound able to inhibit the aorta contractions as well as the calcium release induced by ET-1 via ET_A receptors (*23*). Therefore, by applying a Bpa−scan stategy, we developed six photosensitive probes derived from TTA-386 (*24*). In fact, leucine-1, tryptophane-2, and phenylalanine-6 were substituted successively with D- or L-*p*-benzoyl-phenylalanine (Table 1). The results showed that the radioactive analogues [Tyr(^{125}I)^5, D-Bpa^6]TTA-386 and [Tyr(^{125}I)^5, L-Bpa^6]TTA-386 exhibited functional and binding properties useful for the efficient covalent labeling of human ET_A receptors expressed in transfected CHO cells. This step followed by the fragmentation of the photoligand−receptor complex enabled us to identify a site of the binding domain interacting with the photoprobes.

EXPERIMENTAL PROCEDURES

Materials. Male Sprague−Dawley rats and male Hartley guinea pigs were obtained from Charles River Canada (St-Constant, QC) and kept on a 12-h light−dark cycle with laboratory chow and tap water ad libitum according to standards approved by the Canadian Committee on Animal Care. Boc-L-Bpa and Boc-D-Bpa were purchased from Advanced Chem Tech (Louisville, KY). All other amino acids were obtained from ChemImpex International (Wood Dale, IL) or Albatross (St-Laurent, QC). Benzotriazol-1-yl-oxy-tris(dimethylamino)phosphonium hexafluorophosphate (BOP) was obtained from Albatross. Tetrahydrofuran, DIPEA, homopiperidine, and 4-nitrophenylchloroformate were obtained from Sigma-Aldrich (Mississauga, ON). Chloramine-T, NaI, bovine serum albumin (BSA), protease inhibitor cocktail, anti-endothelin receptor A antibody, CNBr, Endo Lys-C, and V8 protease were also provided by Sigma-Aldrich. The PNGase F kit was obtained from New England BioLabs (Pickering, ON). The Western blot ECL revelation kit, Na^{125}I, and ^{14}C molecular weight standards were purchased from Amersham Biosciences (Montreal, QC). Ham-F12 culture medium, calf serum, and antibiotics were obtained from Biomedia (Drummondville, QC). Recombinant CHO-K1 cell line expressing the human ET_A receptor was obtained from Euroscreen (Brussels, Belgium).

Peptide Synthesis. TTA-386 and its analogues were synthesized using the solid-phase strategy combined with the Boc chemistry methodology. Peptides were assembled on a multireactor system, and chloromethylated resin was used as the solid support. Boc−amino acid couplings were performed in *N*,*N*-dimethylformamide (DMF) in the presence of diisopropylethylamine (DIEA) and BOP as a condensing reagent. TTA-386 (hexamethyleneiminocarbonyl-Leu-D-Trp-D-Ala-βAla-Tyr-D-Phe) and six photosensitive analogues were synthesized by substituting either leucine-1, tryptophane-2, or phenylalanine-6 with a D- or L-Bpa residue (Table 1). Bpa was incorporated into peptides during solid-phase synthesis following the same procedure as for the other amino acid residues. The hexamethyleniminocarbonyl moiety was attached to the free N-terminus of each peptide-resin using 10 equiv of *p*-nitro-phenoxychloroformate diluted in tetrahydrofuran/dichloromethane, in the presence of 1 equiv of DIEA. After 12 h at room temperature, under nitrogen atmosphere, peptide-resins were washed with dichloromethane and DMF. A solution of 20% homopiperidine/DMF was finally added to the peptide-resins, and the reaction was pursued for another 12 h in the same conditions (*25*). Peptides were cleaved from their solid support with hydrogen fluoride (HF) (10 mL g^{-1} resin) using *m*-cresol (1 mL g^{-1} resin) as a scavenger. The reaction was carried out for 60 min at 0 °C. HF was rapidly evaporated, and the resin was washed with anhydrous diethyl ether. Crude synthetic peptides were extracted with trifluoroacetic acid (TFA). After evaporation of TFA, the remaining product was precipitated with diethyl ether. The collected material was dried under vacuum and stored at −20 °C until purification.

Peptide Purification. Crude peptides were purified by means of preparative reverse-phase HPLC using a Jupiter C_{18} column (Phenomenex (CA), 15 μm, 300 Å, 25 cm × 2.12 cm) attached to a Waters Prep LC 500A system equipped with a model 441 absorbance detector (Milford, MA). The material was purified with a 3 h linear gradient from (A) 0.005% ammonium acetate in H_2O, pH 9, to (B) CH_3CN (80%) in 0.005% aqueous ammonium acetate, pH 9. The flow rate was maintained at 20 mL min^{-1}, and detection was at 230 nm. The homogeneity of each fraction was assessed by analytical reverse-phase HPLC. Fractions corresponding to the purified peptides were pooled, lyophilized, and analyzed by mass spectrometry. Purification led to peptide purity equal or superior to 98%, and their molecular mass was confirmed with MALDI-TOF mass spectrometry (Voyager-DE, PerSeptive Biosystems, Foster

City, CA; matrix was the α-cyano-4-hydroxycinnamic acid, accelerating voltage at 20 kV, laser at 337 nm and 20 pulses/s). Peptides in a powder form were kept at −20 °C until biological and biochemical characterizations.

Peptide Iodination with "Cold" Iodine. Iodination of the Tyr^5 residue of each photoprobe was carried out using chloramine-T. Peptides (10 mg) were incubated in a total volume of 10 mL of 0.05 M phosphate buffer (pH 7.4), containing 1.2 equiv of NaI. To favor the production of the monoiodinated or diiodinated peptides, we used 0.5 and 2.0 equiv of chloramine-T, respectively. After 30 s at room temperature, the reaction was stopped by the addition of 400 mg of sodium metabisulfite ($Na_2S_2O_5$) dissolved in 3 mL of sodium phosphate buffer. Monoiodinated peptide was separated from unlabeled and diiodinated peptide by preparative reverse-phase HPLC according to the procedure described previously. Peptide purity was assessed with analytical reverse-phase HPLC, and molecular weight was determined using MALDI-TOF mass spectrometry.

Biological Activity Studies. The antagonistic activity of the TTA-386 derivatives was assessed in two different preparations: rat thoracic aorta rings and guinea pig lung parenchyma strips. Male Sprague−Dawley rats weighing 250−300 g were anesthetized, and the thoracic aorta was rapidly removed and cleaned of fat and connective tissues. The endothelium was removed by gentle rubbing of the intimal surface. Aortas were cut into 4-mm rings and were suspended in 5-mL water-jacketed organ baths containing gassed (95% O_2/5% CO_2) and warmed (37 °C) Krebs−Henseleit solution (120 mM NaCl, 25 mM $NaHCO_3$, 4.7 mM KCl, 1.6 mM $MgSO_4$, 1.17 mM KH_2PO_4, 2.5 mM $CaCl_2$, and 11 mM glucose, at pH 7.4). Rings were stretched to a resting force of 1 g with a 60-min equilibration period. Rings were incubated with various concentrations (3×10^{-8} to 1×10^{-6} M) of TTA-386 or its derivatives. After 15 min, cumulative concentrations (1×10^{-10} to 3×10^{-7} M) of ET were added. Mechanical responses were recorded isometrically on a Grass 7E polygraph with force-displacement transducers (Quincy, MA). The contractile responses were expressed as a percentage of the maximal contractile response produced by KCl (80 mM).

Male Hartley guinea pigs (300−350 g) were anesthetized, and lungs were removed. The parenchyma was dissected in strips that were mounted in the system described above. The antagonistic activity of TTA-386 or its analogues was then measured as above-mentioned. The biological activity was expressed as a percentage of the effect produced after the addition of histamine (10^{-6} M).

Noniodinated, monoiodinated, and diiodinated peptides were tested, and concentration−response curves were analyzed using a nonlinear least-squares regression obtained with the Prism 3.02 software (PRISM, GraphPad Software Inc., San Diego, CA). Results are expressed as mean ± SEM of at least three different experiments, and *n* varied from 8 to 12 animals.

Cell Culture. Chinese hamster ovary (CHO) cells stably expressing the human ET_A receptor were grown at 37 °C with 5% CO_2 in Ham-F12 culture medium supplemented with 10% fetal calf serum, 400 μg mL^{-1} of G418, 100 U mL^{-1} penicillin, 100 μg mL^{-1} streptomycin, and 2.5 μg mL^{-1} fungizone.

Immunoblotting. The molecular weight of the ET_A receptor was determined by an immunoblot analysis. Recombinant hET_A-CHO cells were solubilized in a detergent buffer (50 mM Tris, pH 8, 150 mM NaCl, 0.5% (v/v) Igepal, 0.1% (w/v) SDS, 0.1% (v/v) Triton, and 0.01% (v/v) protease inhibitor cocktail) and submitted to a gentle agitation for 45 min at 4 °C. The solubilized membrane solution was then centrifuged at 16 000*g* for 45 min at 4 °C, and proteins of the supernatant were separated by 10% SDS−PAGE. Proteins were transferred on a PVDF (polyvinylidene fluoride) membrane by electrophoretic blotting, and the ET_A receptor was revealed with an anti-ET_A antibody and a goat-anti-rabbit antibody conjugated to horseradish peroxidase. The receptor was visualized on an X-ray film (Universal X-ray Company of Canada Ltd, Dorval, QC) after an ECL revelation protocol performed according to the procedure from the manufacturer (Amersham Biosciences, Montreal, QC).

Radiolabeling of Peptides. Iodine-125 was incorporated into the tyrosine side chain of TTA-386, [D-Bpa^6]TTA-386 and [L-Bpa^6]TTA-386, using a modified chloramine-T protocol of that described originally by Watakabe (*26*). Peptides (3 nmol) were incubated in a total volume of 150 μL of 0.05 M phosphate buffer (pH 7.4), containing 1 mCi $Na^{125}I$ and 1.5 μg of chloramine-T reagent (5 nmol). After 1 min at room temperature, the reaction was stopped by the addition of 20 μL of sodium metabisulfite (0.1 μg μL^{-1}). The mono [^{125}I]-peptide was separated from unlabeled and diiodinated peptides by analytical reverse-phase HPLC using a Waters 600E system and a Jupiter C_{18} column (5 μm, 300 Å, 250 mm × 4 mm) from Phenomenex. The radioactive material was eluted with a 40-min linear gradient from (A) 30% CH_3CN in 0.06% TFA/H_2O to (B) 70% CH_3CN in 0.06% TFA/H_2O. The flow rate was maintained at 1 mL min^{-1}. Fractions were collected at every 30 s, and the elution pattern was established using a Packard γ-counter (Downers Grove, IL). Radiolabeled peptides were diluted 1:10 in 50 mM sodium phosphate buffer (pH 7.4) and stored at −20 °C. Specific activity was assumed to be at 2200 Ci/mmol.

Binding Assays. The day before the experiment, recombinant hET_A-CHO cells were seeded in 12-well tissue culture plates at a density of 2.5×10^5 cells/well. The next day, cells at almost 90% confluency were rinsed twice with cold washing buffer (50 mM Tris-HCl, pH 7.4, 5 mM $MgCl_2$, and 100 mM NaCl). Cells (≅ 20 μg of proteins/well) were incubated at 4 °C for 16 h with 1 nM of [$Tyr(^{125}I)^5$]TTA-386, [$Tyr(^{125}I)^5$, D-Bpa^6]TTA-386, or [$Tyr(^{125}I)^5$, L-Bpa^6]-TTA-386 in the presence of increasing concentrations of five unlabeled competitors: ET-1, BQ-610, TTA-386, [D-Bpa^6]-TTA-386, and [L-Bpa^6]TTA-386 in a final volume of 0.5 mL. Binding assays with whole attached cells were performed in binding buffer (50 mM Tris-HCl, pH 7.4, 5 mM $MgCl_2$, 100 mM NaCl, 0.001% (w/v) BSA, and 0.01% (v/v) protease inhibitor cocktail containing AEBSF, aprotinin, leupeptin, bestatin, pepstatin A ,and E-64. After incubation, cells were washed twice with cold washing buffer and solubilized in 1 N NaOH, and cell-bound radioactivity was evaluated by γ counting. The IC_{50} values for the various competitors were determined by using the GraphPad Prism 3.02 software. Results are expressed as mean ± SEM of three independent assays carried out in duplicate.

Photoaffinity Labeling. The day before the experiment, recombinant hET_A-CHO cells were seeded in 35 mm dishes

at a density of 5×10^5 cells/dish. The next day, cells at almost 90% confluency were rinsed twice with cold washing buffer. Cells (≅ 40 μg of proteins/well) were incubated at 4 °C for 16 h in 750 μL of binding buffer containing 5 nM of [Tyr(^{125}I)^5, D-Bpa^6]TTA-386 or [Tyr(^{125}I)^5, L-Bpa^6]TTA-386, in the presence or absence of 1 μM ET-1 or 1 μM BQ-610, an ET_A selective antagonist. Cells were washed twice with washing buffer and then irradiated with UV (100 W lamp, 365 nm) for 1 h at 0 °C, at a distance of 6 cm. Afterward, 750 μL of the detergent buffer was added, and cells were gently scraped and solubilized. Cells were further submitted to a gentle agitation for 45 min. The solutions were then centrifuged at 16 000*g* for 45 min at 4 °C. The supernatants were stored at −20 °C until further analysis.

Identification of the Labeled Complex. The solubilized photolabeled receptors were diluted 1:2 with a loading buffer (62.5 mM Tris-HCl, pH 6.8, 20% (v/v) glycerol, 2% (w/v) SDS, 5% (v/v) β-mercaptoethanol, and 0.025% (w/v) bromophenol blue) and incubated for 1 h at 37 °C. A 10% SDS−PAGE was performed using a 1 mm-thick gel. After a migration at 175 V for 1 h, the gels were dried on filter papers and exposed to X-ray film with an intensifying screen. [^{14}C]Methylated molecular standards (14−220 kDa) were used to determine the molecular mass of the radiolabeled complex.

Partial Purification of the Photolabeled Complex. The solubilized photolabeled receptors were diluted 1:2 with the loading buffer described above and incubated for 1 h at 37 °C. A 10% SDS−PAGE electrophoresis was performed using a 1.5 mm-thick gel. The gel was then cut into slices, and their radioactive content was measured with a γ-counter. The labeled receptor was electroeluted from the gel slices into electroelution buffer (25 mM Tris base, 192 mM glycine, and 0.1% SDS) for 3.5 h at room temperature as recommended by the electroelution apparatus protocol of the manufacturer (Bio-Rad, Mississauga, ON). The eluate was concentrated to a final volume of 30 μL using Centricon-10 and was stored at −20 °C.

Endoglycosidase, Proteolytic, and Chemical Digestions. Concentrated proteins from hET_A-CHO cells were resuspended in a denaturing buffer and incubated with PNGase-F for 3 h at 37 °C, as described by the manufacturer (New England BioLabs). For CNBr cleavage, the partially purified photolabeled receptors were resuspended in 200 μL of 50% (v/v) TFA/H_2O before adding 200 μL of ACN containing 50 mg of CNBr. The samples were incubated at room temperature, in the dark for 16−18 h. The reaction was terminated by adding 3 mL of water. Samples were lyophylised twice to remove most of the salts. For proteolytic digestions, partially purified photolabeled receptors were digested for 16−20 h at 37 °C with 1 μg of Endo Lys-C protease in 25 μL of digestion buffer containing 25 mM Tris-HCl, pH 8, 1 mM EDTA, and 0.1% SDS. Partially purified receptors were also digested for 7 days at room temperature with 8 μg of V8 protease in 25 μL of buffer containing 100 mM ammonium carbonate, pH 8, and 0.1% SDS. All digestions were terminated by addition of an equal volume of loading buffer followed by an incubation at 37 °C for 1 h.

Analysis of Products of Proteolysis and Chemical Cleavage. The products of proteolysis and chemical cleavage were analyzed by SDS−PAGE using 16.5% Tris-Tricine gels. After a migration at 80 V for 4 h, the gels were dried on filter paper and exposed to X-ray film with an intensifying screen. ^{14}C-Labeled low-molecular protein standards (5−30 kDa) were used to determine the molecular mass of the photolabeled fragments.

Table 1: TTA-386 Synthetic Analogues[a]

peptides	primary sequences
TTA-386	homopiperidinyl-CO-Leu-D-Trp-D-Ala-βAla-Tyr-D-Phe
[d-Bpa^1]-TTA-386	homopiperidinyl-CO-**Bpa**-D-Trp-D-Ala-βAla-Tyr-D-Phe
[L-Bpa^1]-TTA-386	homopiperidinyl-CO-**Bpa**-D-Trp-D-Ala-βAla-Tyr-D-Phe
[D-Bpa^2]-TTA-386	homopiperidinyl-CO-Leu-**Bpa**-D-Ala-βAla-Tyr-D-Phe
[L-Bpa^2]-TTA-386	homopiperidinyl-CO-Leu-**Bpa**-D-Ala-βAla-Tyr-D-Phe
[D-Bpa^6]-TTA-386	homopiperidinyl-CO-Leu-D-Trp-D-Ala-βAla-Tyr-**Bpa**
[L-Bpa^6]-TTA-386	homopiperidinyl-CO-Leu-D-Trp-D-Ala-βAla-Tyr-**Bpa**

[a] As described in Experimental Procedures, TTA-386 and its analogues were synthesized using a solid-phase peptide synthesis strategy combined with the Boc chemistry methodology. The urea moiety was introduced at the N-terminus of each peptide-resin using 10 equiv of *p*-nitro-phenylchloroformate in the presence of 1 equiv DIPEA. After 12 h of reaction at room temperature, under nitrogen, a solution of 20% homopiperidine/DMF was added to the peptide-resins, and the reaction was pursued for another 12 h.

RESULTS

Peptide Synthesis and Purification. Table 1 shows the amino acid sequences of the specific ET_A receptor antagonist, TTA-386, and six photosensitive analogues. The amino acids Leu^1, D-Trp^2, and D-Phe^6 were replaced successively with a D- or L-Bpa residue. The photoprobes were assembled with the so-called Boc chemistry protocol, using BOP as the coupling reagent. As a final step, the addition of the urea cycle at the N-terminus of each peptide was then performed by the incorporation of a *p*-nitrophenoxycarbonyl moiety followed by an aminolysis using homopiperidine. The reaction with *p*-nitrophenoxyde chloroformate was monitored with the Kaiser test, and it demonstrated the absence of remaining free N-terminus in peptides. The extent of the first reaction with *p*-nitrophenyl chloroformate was also checked by HPLC after cleaving an aliquot of peptide-resin. As shown in Figure 1A,B, an overnight treatment gave a single peak, exhibiting a slightly more hydrophobic character than the parent compound (17 min versus 16.3 min). Furthermore, a MALDI-TOF mass spectrometry analysis confirmed the N-terminal introduction of the *p*-nitrophenoxycarbonyl group. Similarly, the aminolysis step was also monitored by HPLC after cleaving a peptide-resin aliquot. As depicted in Figure 1C (the aminolysis product) and Figure 1D (coinjection of the *p*-nitrophenoxycarbonyl peptide and the homopiperidinyl derivative), the 12-h reaction of homopiperidine with the activated *p*-nitrophenyl ester gave a single product different to the starting material. Mass spectrometry analysis confirmed the presence of the urea moiety at the N-terminus of the TTA-386 analogues. Purity of the final peptides (≥98%) was assessed by analytical HPLC.

Pharmacological Studies. The biological activity of the photoprobes was measured in the rat thoracic aorta and guinea pig lung parenchyma bioassays, two pharmacological preparations showing predominant populations of ET_A and ET_B receptors, respectively. Figure 2 shows the concentration−response curves of ET-1 in the presence of growing concentrations of the photosensitive analogues. In isolated endothelium-denuded rat aortic rings, two of the photoprobes synthesized, [D-Bpa^6]TTA-386 and [L-Bpa^6]TTA-386, pro-

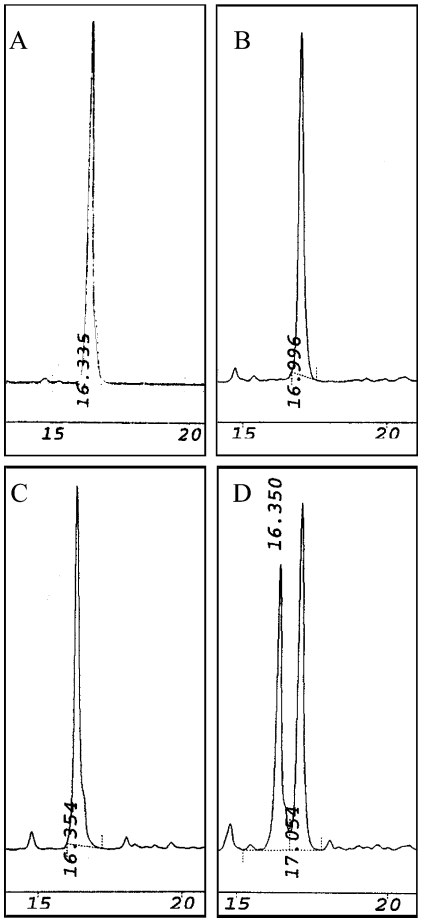

FIGURE 1: Analytical HPLC chromatograms of [D-Bpa^6]TTA-386 during its synthesis: (A) [des-homopiperidinylcarbonyl, D-Bpa^6]-TTA-386; (B) compound A after its reaction with *p*-nitrophenoxychloroformate; (C) compound B after treatment with homopiperidine; and (D) coinjection of compounds B and C on a reverse-phase HPLC using a Vydac C_{18} column (5 μm, 300 Å; 250 mm × 4 mm) with a 30-min linear gradient of acetonitrile (40−70%) in 0.06% aqueous TFA.

duced a parallel rightward shift of the ET-1 concentration−response curves in a concentration-dependent manner. These peptides did not show any agonistic effect and did not exhibit any significant changes in the maximal responses. A nonlinear regression yielded a similar pA_2 value on rat aortic rings for TTA-386 (7.9) and its two antagonist analogues [D-Bpa^6]TTA-386 (7.5) and [L-Bpa^6]TTA-386 (7.7). However, the substitution with Bpa of Leu^1 and Trp^2 of TTA-386 resulted in a complete loss of affinity on ET_A receptors. In addition, none of the six photoprobes produced a potent biological effect, neither agonist nor antagonist, in the lung parenchyma, suggesting that the active probes were still highly selective for the ET_A receptor.

Radioiodination of the probes is an essential step to subsequently allow the visualization of the photolabeled receptor. Hence, a second series of pharmacological activity was evaluated with the probes after iodination with "cold" iodine to confirm that the incorporation of this atom into the phenolic ring of Tyr^5 did not abolish the affinity of the TTA-386 derivatives. Bioassays on rat aorta demonstrated that the pharmacological properties of the new antagonists [D-Bpa^6]TTA-386 and [L-Bpa^6]TTA-386 are modulated by the presence of one or two iodine atoms on the tyrosine-5 residue. As shown in Figure 3A, monoiodinated or diiodinated [L-Bpa^6]TTA-386 produced a parallel rightward shift of the ET-1 concentration−response curve. Nevertheless, a decrease in the antagonist activity of the iodinated peptide was observed when compared with the ET-1 concentration−response curve in the presence of the noniodinated peptide. Iodination of this peptide did not affect its selectivity toward the ET_A receptor because it remained inactive in the guinea pig lung parenchyma paradigm. Surprisingly though, monoiodination of [D-Bpa^6]TTA-386 produced a weak agonist activity on the rat thoracic aorta, while being inactive on ET_B receptors (Figure 3B). Furthermore, the addition of a second iodine atom in this peptide led to the recovery of an antagonistic activity, slightly less potent than that of the noniodinated counterpart (Figure 3C).

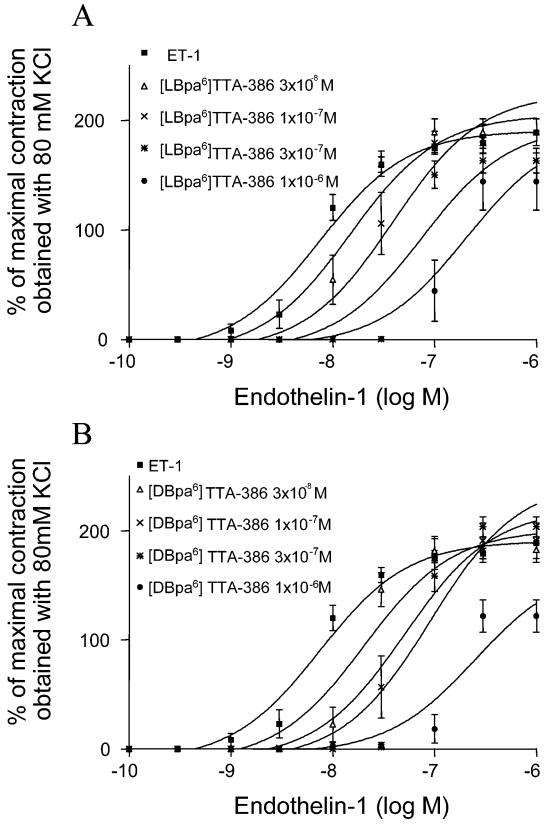

FIGURE 2: Concentration−response curves of ET-1 in the presence of increasing concentrations of [L-Bpa^6]TTA-386 (A) or [D-Bpa^6]-TTA-386 (B) obtained in isolated endothelium-denuded rat aortic rings (ET_A preparation). Results are expressed as percentage of the contractile response induced with 80 mM KCl.

Binding Assays. Intact CHO cells expressing the human ET_A receptor (Figure 4) were used to assess the affinity potencies of the photoprobes showing pharmacological properties. Affinity assessment was carried out by competitive binding assays using [^{125}I-Tyr^5, D-Bpa^6]TTA-386 and [^{125}I-Tyr^5, L-Bpa^6]TTA-386 as tracers. As shown in Figure 5, both analogues were able to bind to receptors and were displaced in the presence of either of the five competitors, ET-1, BQ-610 (a specific ET_A receptor antagonist), TTA-386, [D-Bpa^6]TTA-386, and [L-Bpa^6]TTA-386. The IC_{50} values are given in Table 2. These data suggested that the two radioligands possess a good affinity for ET_A receptors and share the same binding site of ET_A receptors. Unexpectedly, ET-1 was the less efficient competitor for both radioligands. Moreover, ET-1 was unable to completely displace the tracers as demonstrated by the high percentage

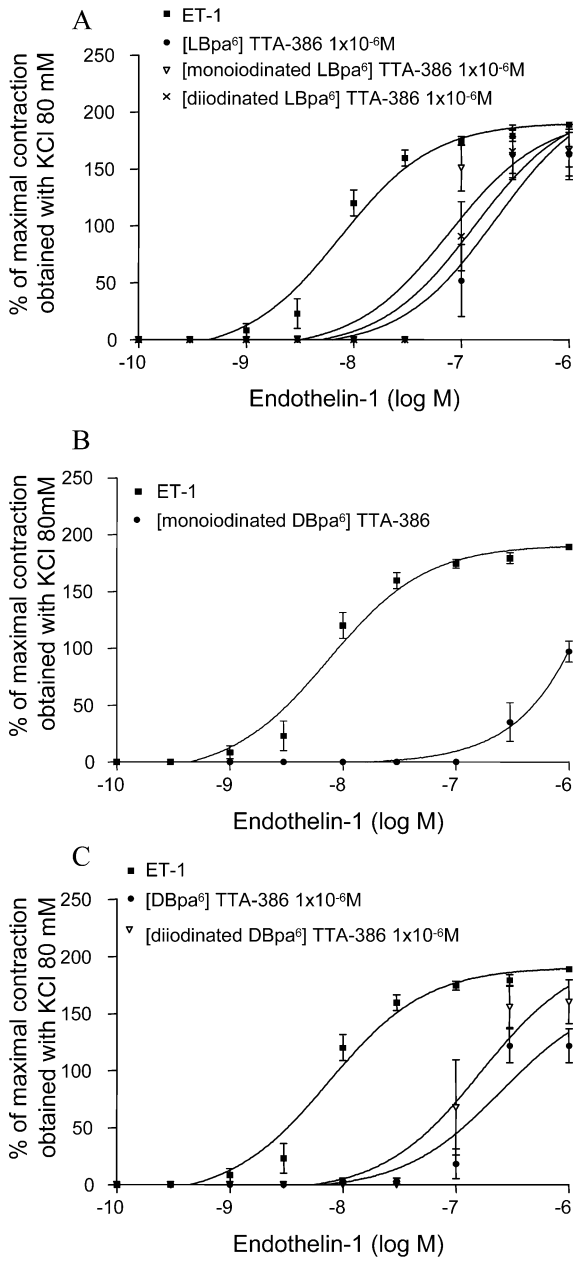

FIGURE 3: Concentration−response curves of ET-1 in the presence of 1 μM of noniodinated, mono-, and diiodinated [L-Bpa^6]TTA-386 (A), concentration−response curves of ET-1 and monoiodinated [D-Bpa^6]TTA-386 (B), and concentration−response curves of ET-1 in the presence of 1 μM of noniodinated and diiodinated [D-Bpa6]-TTA-386 (C). All these concentration−response curves were obtained in isolated endothelium-denuded rat aortic rings (ET_A preparation). Results are expressed as percentage of the contractile response induced with 80 mM KCl.

of remaining radioactivity bound to the cells. Nevertheless, the binding experiments demonstrated that both radioligands exhibited an excellent affinity for ET_A receptors and probably shared the same binding site as ET-1. They were then favored for photoaffinity labeling.

Photoaffinity Labeling of ET_A Receptors. As shown with a 10% SDS−PAGE analysis, photoactivation of [^{125}I-Tyr^5, D-Bpa^6]TTA-386 and [^{125}I-Tyr^5, L-Bpa^6]TTA-386 bound to ET_A receptors found at the surface of CHO cells resulted in their covalent attachment (Figure 6A, lanes 1 and 4; ≈70 kDa complex). Furthermore, the formation of the complex between [^{125}I-Tyr^5, D-Bpa^6]TTA-386 or [^{125}I-Tyr^5, L-Bpa^6]-TTA-386 and the receptor was completely abolished in the presence of ET-1 (lane 2) or BQ-610 (lane 3) demonstrating the specificity of the labeling. In addition, the identity of the ET_A receptor was confirmed by immunoblotting experiments that showed that the 60−70 kDa protein was recognized by antibodies raised against the ET_A receptors (Figure 6B, lane 1). Thus, the 60 kDa photolabeled protein would be the mass of the photosensitive ligands (1125 Da) linked to the glycosylated ET_A receptor (60−70 kDa) since a PNGase F treatment (an enzyme that cleaves asparagine-linked carbohydrates) reduced the receptor mass to 48 kDa, a molecular mass consistent with that calculated from the ET_A receptor sequence (Figure 6B, lane 2).

Analysis of Proteolytic Products and Chemical Cleavages. To identify the binding domain, the ET_A receptor photolabeled with either photoprobe was partially purified by SDS−PAGE and submitted to Endo Lys-C digestion, an enzyme cleaving at the C-terminal side of lysine residues. This enzymatic cleavage produced on a 16.5% acrylamide−tris-tricine separating gel, a well-resolved fragment at 5.9 kDa (Figure 7A, lane 3) that would correspond to the smallest digestion fragment of the receptor photolabeled with the photoligands. Since the iodinated photoprobes have a mass of 1125 Da, then the photolabeled segment would possess a molecular weight at around 4.8 kDa. A computerized analysis with the Peptide Mass software, of the ET_A receptor sequence and of its fragments produced after complete and partial Endo Lys-C digestion, identified four peptide segments Cys^{110}−Lys^{159} (5.5 kDa), Asp^{256}−Lys^{299} (5.3 kDa), Gln^{300}−Lys^{338} (4.8 kDa), and Asn^{339}−Lys^{377} (4.5 kDa) corresponding to a possible segment of the binding domain of ET_A. Except for the second suggestion, the other fragments would be produced after an incomplete digestion by the enzyme (Figure 7B).

To further define the labeled region, we proceeded to an alternative digestion step of the photolabeled complex with V8, an enzyme that cleaves peptide bonds on the carboxylic side of aspartate and glutamate residues. Again, multiple bands were observed, thus, suggesting an incomplete digestion (Figure 8A, lane 4). Nevertheless, the analysis of the bands revealed that the shortest fragment exhibiting a mass of 4 kDa corresponded to the sum of the photoprobe mass (1.1 kDa) and that of the photolabeled segment (2.9 kDa). According to the analysis of the primary structure of the ET_A receptor, five fragments could match these mass data, that is, Leu^{127}−Asp^{152} (3.1 kDa), Phe^{153}−Asp^{182} (3.3 kDa), Ile^{206}−Glu^{230} (2.8 kDa), Gln^{235}−Asp^{256} (2.7 kDa), and Trp^{257}−Glu^{281} (3.1 kDa) (Figure 8B). Except for the last segment, the others would be produced after an incomplete digestion by the enzyme. As mentioned above and demonstrated by the number of bands observed on the gel, even a prolonged V8 treatment (7 days) did not lead to a complete digestion. However, by combining the Endo Lys-C and V8 digestion results, we can reject the possibility that the V8 fragments Ile^{206}−Glu^{230} and Gln^{235}−Asp^{256} are parts of the binding domain because none of the expected proteolytic fragments showed any overlaps. Similarly, the Endo Lys-C fragments Gln^{300}−Lys^{338} and Asn^{339}−Lys^{377} must also be rejected as parts of the binding domain. Thus, taking into account that the labeled sequences produced by the two different enzymatic digestions must overlap, two binding domains can be identified. The ET_A binding domain then

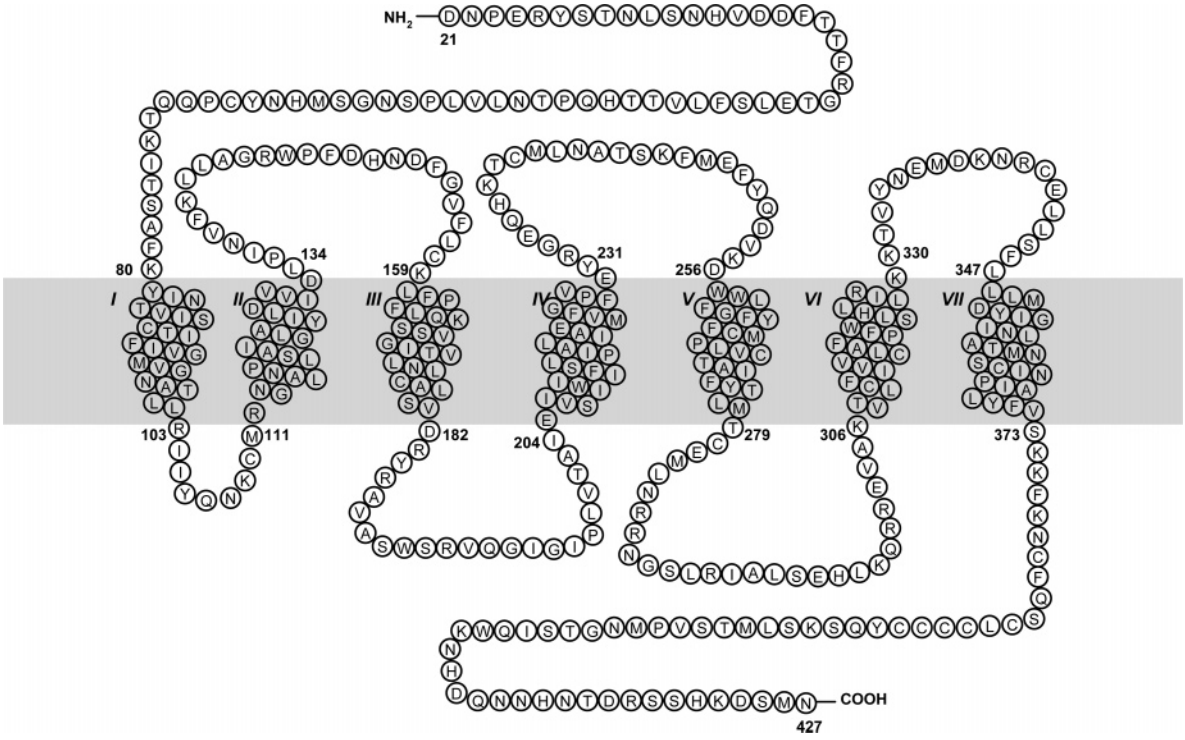

FIGURE 4: Primary structure of the human ET_A receptor.

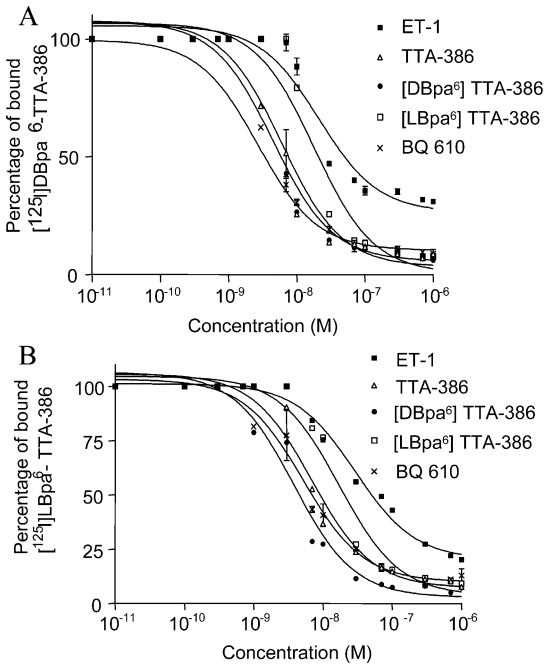

FIGURE 5: Competitive displacement of [D-Bpa^6]TTA-386 (A) and [L-Bpa^6]TTA-386 (B) bound to CHO-ET_A cells using unlabeled ET-1, TTA-386, BQ-610, [D-Bpa^6]TTA-386, and [L-Bpa^6]-TTA-386 as competitors. The IC_{50} values for the displacement of the radioiodinated photoprobes are summarized in Table 2. The data are shown as a percentage of the specific control binding determined in the absence of competing ligands and are representative of three to five similar independent experiments carried out in duplicate.

would be located either in the first extracellular loop between residues Leu^{127} and Asp^{152} or in the fifth transmembrane domain between residues Trp^{257} and Glu^{281}.

To further confirm the labeling site, we proceeded to a chemical treatment with CNBr that cleaves at the carboxylic side of methionine residues. The analysis of the fragment appearing on the gel just before some residual free ligand revealed a mass of 5 kDa that would be the sum of the photoprobe mass (1.1 kDa; Figure 9A, lane 3) and that of the photolabeled fragment (3.9 kDa) (Figure 9A, lane 4). On the basis of this latter mass, only one stretch, corresponding to Glu^{249}−Met^{278} (3.7 kDa) can fulfill the entire data (Figure 9B). In addition, it also strongly suggests that the photocoupling to the receptor did not proceed through a Met side chain because, in such a case, the CNBr cleavage would have essentially produced a fragment exhibiting the mass of the photoprobe. Finally, it can be pinpointed that a PNGase F treatment before the enzymatic and chemical digestions of the receptor did not modify the mass of labeled fragments obtained.

Table 2: IC_{50} Values Measured with Competition Binding Assays, Using [Tyr(^{125}I), D-Bpa^6]TTA-386 or [Tyr(^{125}I), L-Bpa^6]TTA-386 as Tracers and Intact CHO Cells Expressing the Human ET_A Receptors[a,b]

competing peptides	IC_{50} values (nM)	
	[Tyr(^{125}I), D-Bpa^6]TTA-386	[Tyr(^{125}I), L-Bpa^6]TTA-386
ET-1	21 ± 8	29 ± 8
BQ-610	3.0 ± 0.5	5.2 ± 0.7
[D-Bpa^6]TTA-386	6.1 ± 0.6	3.8 ± 0.7
[L-Bpa^6]TTA-386	18 ± 6	17 ± 7
TTA-386	4.5 ± 0.7	6.9 ± 0.8

[a] Recombinant hET_A-CHO cells were incubated at 4 °C for 12 h with 1 nM of [Tyr^5(^{125}I), D-Bpa^6]TTA-386 or [Tyr^5(^{125}I), L-Bpa^6]-TTA-386 in the presence of increasing concentrations of five unlabeled competitors: ET-1, BQ-610, TTA-386, [D-Bpa^6]TTA-386, and [L-Bpa^6]TTA-386. After incubation, cells were washed twice with cold washing buffer and solubilized in 1 N NaOH, and cell-bound radioactivity was evaluated with γ-counting as described in Experimental Procedures. [b] The other monosubstituted TTA-386 derivatives were devoid of affinity. Therefore, they were not included in the competition studies.

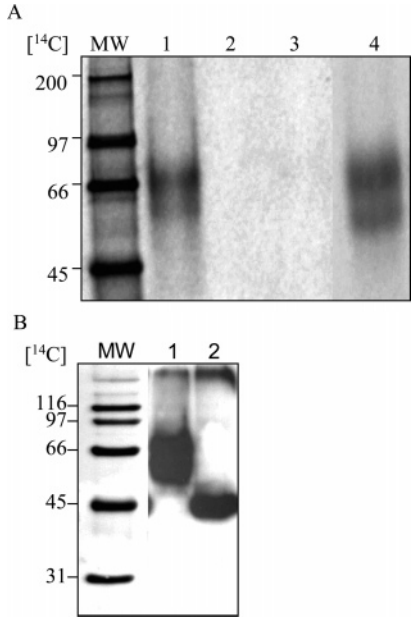

FIGURE 6: ET_A receptor analysis by SDS−PAGE. (A) Specific photolabeling of ET_A receptors with [Tyr(125I), D-Bpa6]TTA-386 (lane 1) and [Tyr(125I), L-Bpa6]TTA-386 (lane 4). CHO cells transfected with ET_A receptors were photolabeled with these probes as described in the experimental section. CHO cells expressing the ET_A receptor were equilibrated with 5 nM of one of these ligands, in the dark at 4 °C for 12 h, either alone or in the presence of 1 μM ET-1 (lane 2) or BQ-610 (lane 3). Membrane proteins were solubilized and then analyzed with SDS−PAGE. (B) Immunoblot analysis of ET_A receptors. Identification of the ET_A receptor transfected in CHO cells before (lane 1) and after PNGase F treatment (lane 2). Protein standards of the indicated molecular masses (in kDa) were run in parallel. These results are representative of at least three separate experiments.

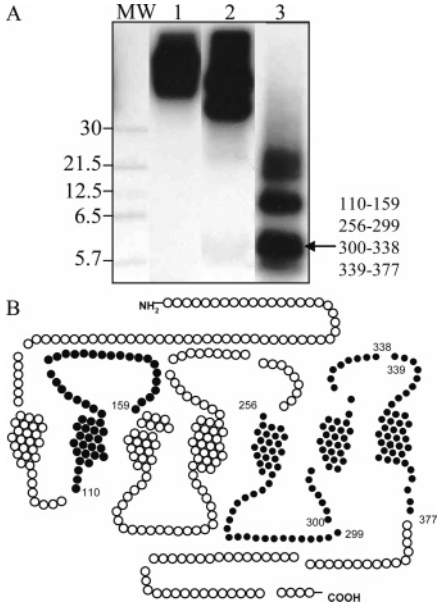

FIGURE 7: Endo Lys-C digestion of ET_A receptors photolabeled with [Tyr(125I), D-Bpa6]TTA-386 or [Tyr(125I), L-Bpa6]TTA-386 (both give the same SDS−PAGE pattern). (A) Partially purified photolabeled ET_A receptors were incubated in the absence (lane 1) or in the presence of 1 μg Endo Lys-C (lane 3) at 37 °C for 18 h. All samples were run on a 16.5% acrylamide−tris-tricine separating gel followed by autoradiography. 14C-Labeled protein standards were run in parallel. These results are representative of at least three separate experiments. (B) Representation of the ET_A receptor showing, in black closed circles, five possible fragments that could be bound to the photolabile ligands after the Endo Lys-C digestion.

DISCUSSION

The identification of the molecular determinants involved in the affinity of a ligand to its receptor is an essential step to understand the activation process. To reach this goal, photoaffinity labeling appears as a useful strategy for exploring the binding area within a receptor. This approach requires the development of radioactive photoligands able to form with the receptor protein a covalent conjugate that can be mapped subsequently. Hence, we prepared six photosensitive probes derived from the specific ET_A antagonist TTA-386 in which the hydrophobic residues L-leucine-1, D-tryptophan-2 and D-phenylalanine-6 were successively substituted with a D- or L-Bpa residue. The other hydrophobic amino acid, L-tyrosine-5, was conserved because of its usefulness for radiolabeling.

The synthesis of TTA-386 and its analogues was carried out using standard solid-phase procedures with BOP as an activating reagent for the amino acid couplings. For the last step consisting in the introduction of the urea moiety, activation of the free N-terminus was accomplished with *p*-nitrophenoxychloroformate. This reaction produced a *p*-nitrophenol-derived active ester that, after treatment with homopiperidine, generated the hexamethyleneiminocarbonyl group. This approach was successful and gave a single product. Other methodologies were explored for the incorporation of the N-terminal cyclic urea. For instance, instead of activating the N-terminal amino group of the peptide linked to the solid phase, we verified the feasibility of producing a reactive homopiperidine derivative able to couple to the N-terminus of the peptide chain still linked to the solid phase. So far, reactions of homopiperidine with disuccinimidyl carbonate, phosgene, carbonyldiimidazole, or *p*-nitrophenoxychloroformate were checked for their efficacy. However, none of the activated homopiperidine derivatives were able to give a yield of incorporation of the hexamethyleneiminocarbonyl group, in the peptide chain, as good as that obtained after N-terminal activation followed by a homopiperidine treatment.

The synthetic peptides were then characterized for their capacity to selectively recognize the ET_A receptor. We observed, with ET_A and ET_B paradigms, that the first and second residues of TTA-386 cannot be substituted with D- or L-Bpa because [D- or L-Bpa1]TTA-386 and [D- or L-Bpa2]-TTA-386 were completely devoid of antagonistic activity. The reasons for that loss of affinity were not studied. Nevertheless, it is clear that hydrophobicity is not the only pharmacophoric parameter required by positions 1 and 2 to confer affinity to TTA-386 toward the ET_A receptor. Nonetheless, an antagonist activity was obtained with analogues [D-Bpa6]TTA-386 and [L-Bpa6]TTA-386, two analogues in which Bpa replaced the D-phenylalanine amino acid. Their analogous structure is probably the key factor explaining the maintenance of a potent antagonistic effect with these peptides. Furthermore, the stereochemistry of the Bpa residue did not affect the peptides activity, and as such, pA_2 values of 7.5 and 7.7 were calculated for [D-Bpa6]TTA-386 and [L-Bpa6]TTA-386, respectively. Therefore, considering their antagonistic ability, we can postulate that [D-Bpa6]-TTA-386 and [L-Bpa6]TTA-386 adopt a similar binding conformation to that of TTA-386. Moreover, it also suggested

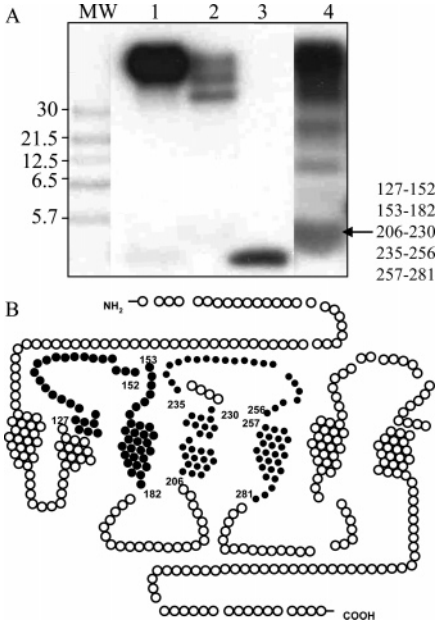

FIGURE 8: V8 protease digestion of ET_A receptors photolabeled with [Tyr(^{125}I), D-Bpa^6]TTA-386 or [Tyr(^{125}I), L-Bpa^6]TTA-386 (both give the same SDS−PAGE pattern). (A) Partially purified photolabeled ET_A receptors were incubated in the absence (lane 1) or in the presence of 8 μg of V8 protease (lane 4) at room temperature for 7 days. The radiolabeled probes (lane 3) were also loaded on the gel. The samples were run on a 16.5% acrylamide−tris-tricine separating gel followed by autoradiography. ^{14}C-Labeled protein standards were run in parallel. These results are representative of at least three separate experiments. (B) Representation of the ET_A receptor showing, in black closed circles, five possible fragments that could be bound to the photolabile ligands after the V8 protease digestion.

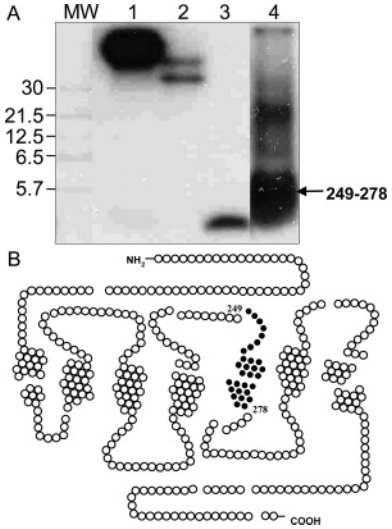

FIGURE 9: CNBr cleavage of ET_A receptors photolabeled with [Tyr(^{125}I), D-Bpa^6]TTA-386 or [Tyr(^{125}I), L-Bpa^6]TTA-386. (A) Partially purified photolabeled ET_A receptors were incubated in the absence (lane 1) or in the presence of CNBr (125 mg/mL) (lane 4) at room temperature for 18 h in the dark. The radiolabeled probes (lane 3) were also loaded on the gel. The samples were run on a 16.5% acrylamide−tris-tricine separating gel followed by autoradiography. ^{14}C-Labeled protein standards were run in parallel. These results are representative of at least three separate experiments. (B) Representation of the ET_A receptor showing, in black closed circles, one possible fragment that could be bound to the photolabile ligands after the CNBr cleavage.

that residue 6 of those molecules is localized in a region of the binding pocket where the amino acid side chain exhibits some freedom in its movement.

Because the probes need to be radiolabeled for their detection on SDS gel after photoactivation, we verified if the presence of one or two iodine atoms on the peptides modified their pharmacological profile on the ET_A receptor. The lactoperoxidase and iodogen techniques are frequently used for peptides iodination. However, these two reagents are usually utilized to iodinate small amounts of peptides. Because the biological analyses that we had planned to perform would require about 2 mg of peptides, iodination of the two antagonist photolabile peptides was carried out using chloramine-T as an oxidizing reagent. Both iodinated analogues (mono and di) were isolated by RP-HPLC, and their pharmacological studies in isolated endothelium-denuded rat aortic rings revealed that the photosensitive probe [L-Bpa^6]TTA-386 under its mono- or diiodinated form, was still able to bind the ET_A receptor and block the effect of endothelin. In fact, the introduction of the iodine atoms had almost no effects on the affinity, and only a slight decrease of antagonistic activity was measured with both peptides.

The [D-Bpa^6]TTA-386 molecule also showed a similar antagonistic pattern after diiodination. However, instead of giving an antagonist, monoiodination produced an analogue with an agonistic activity on ET_A receptors (apparent EC_{50} at 3×10^{-7} M). To the best of our knowledge, this is the first case described in the literature where the activity of a peptide is reversed by its monoiodination. It is yet unclear why the introduction of one iodine atom into the tyrosine side chain gave rise to an agonist, while the incorporation of a second iodine atom brought back the antagonistic properties. This phenomenon cannot be related to the hydrophobicity or ionization state of the phenolic moiety of Tyr-5, because the tyrosine side chain is more hydrophobic with two iodine atoms than with only one and the decrease of the pK_a value is more pronounced in the former case. Therefore, it appears that monoiodination of [D-Bpa^6]TTA-386 would change the peptide structure and allow a key interaction (or key interactions) leading to the ET_A receptor activation. It is however obvious that D-Bpa is an essential feature for developing the agonistic effect because monoiodination of TTA-386, in which position 6 is occupied with D-Phe, did not behave as an agonist (data not shown). Therefore, we postulated that the introduction of one meta-iodine atom into the Tyr-5 residue, in combination with the presence of a bulky benzoylphenyl group in the proper configuration, probably modified the orientation of the tyrosine-5 side chain in such a way that the phenolate function can induce a biological response. This hypothesis is actually under evaluation.

Competitive assays using radiolabeled [D-Bpa^6]TTA-386 or [L-Bpa^6]TTA-386 revealed a similar affinity for ET_A receptors. Also, both of them appeared selective because they can be displaced by five different ET_A ligands. When used in photolabeling experiments performed in transfected CHO cells, [D-Bpa^6]TTA-386 and [L-Bpa^6]TTA-386 specifically labeled a protein that migrated as a diffuse band spanning between 60 and 70 kDa on SDS−PAGE. The 60−70 kDa band that was obtained, corresponding to a complex formed by a protein covalently attached to [D-Bpa^6]TTA-386 or [L-Bpa^6]TTA-386, was shown to be superimposable to an ET_A receptor band identified by immunoblotting assays,

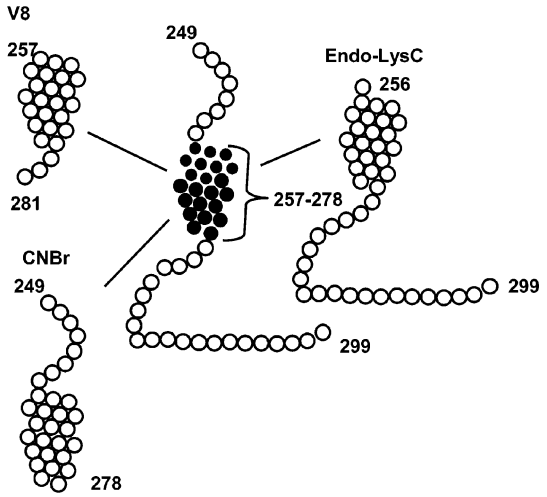

FIGURE 10: Schematic representation of the labeled domain of the ET_A receptor after covalent bonding with [Tyr(^{125}I), D-Bpa^6]-TTA-386 or [Tyr(^{125}I), L-Bpa^6]TTA-386. According to the CNBr cleavage, as well as the Endo Lys-C and V8 protease digestions, the receptor residues 257−278 would form the common fragment.

using anti-ET_A polyclonal antibodies. Moreover, excess of ET-1 or BQ 610 abolished the photolabeling, demonstrating that the two probes compete for the same binding site. Although the theoretical molecular mass of the ET_A receptor is 48 kDa, the visualization of the same band with an anti-ET_A receptor antibody suggested that the photosensitive peptides labeled this receptor. As a matter of fact, a previous PNGase F treatment of cell proteins before the revelation with the antibody showed a protein migrating at around 48 kDa on SDS−PAGE. Thus, the diffuse appearance of the 60−70 kDa band, as well as its susceptibility to PNGase F treatment, confirmed the glycosylated nature of the receptor, a phenomenon frequently encountered (*22*, *27*).

To better define the binding site of [D-Bpa^6]TTA-386 and [L-Bpa^6]TTA-386 on ET_A receptors, the photolabeled complexes were cleaved using either Endo Lys-C protease, V8 protease, or CNBr in the presence or in the absence of PNgase F. According to the selectivity of these enzymatic or chemical treatments and considering that radiolabeled fragments produced by them must overlap, the 4.8 kDa segment formed after Endo Lys-C treatment would be composed of residues Asp^{256}−Lys^{299}, the 2.9 kDa fragment of V8 protease would be Trp^{257}−Glu^{281}, and CNBr would have produced the fragment Glu^{249}−Met^{278} with a mass of 3.9 kDa. Fragments obtained after the cleavage were unchanged even when the receptor was under its deglycosylated form, demonstrating that the binding domain is not glycosylated. Taken together, these data clearly identify a common sequence of 2.7 kDa that would correspond to residues Trp^{257} and Met^{278} (Figure 10). Thus, this cell surface-oriented segment of the fifth transmembrane domain of the ET_A receptor would play an important role in the binding of the photoprobes [D-Bpa^6]TTA-386 and [L-Bpa^6]TTA-386. Therefore, it appears that both would share the same binding site. Moreover, these data are validated by the fact that an excess of ET-1 or BQ-610 abolished the photolabeling of the ET_A receptor produced with [D-Bpa^6]TTA-386 or [L-Bpa^6]-TTA-386, respectively. Interestingly, a recent photolabeling study of the ET_B receptor, carried out with IRL-1620-derived photoprobes specific for this receptor, also identified a stretch of TM V as a key-feature for the interaction between the ET receptor and its ligands (*28*).

In conclusion, using the photoaffinity labeling technique, we have identified a key segment of the ET_A receptor participating in the interaction with the ET-1 or TTA-386 ligands. This protocol had the advantage that an unaltered form of the receptor, as obtained for instance with the site-directed mutagenesis technique, was explored. Further structural and binding data will however be required to complete the molecular dissection of the ET_A binding pocket.

ACKNOWLEDGMENT

The authors thank Myriam Létourneau, Chantal Langlois, Steve Bourgault, and Alexandra Louimaire for their assistance and proof-reading.

REFERENCES

1. Yanagisawa, M., Kurihara, H., Kimura, S., Tomobe, Y., Kobayashi, M., Mitsui, Y., Yazaki, Y., Goto, K., and Masaki, T. (1988) A novel potent vasoconstrictor peptide produced by vascular entothelial cells, *Nature 332*, 411−415.
2. Mateo, A. O., and DeArtinano, A. (1997) Highlights on endothelins: a review, *Pharmacol. Res. 36*, 339−351.
3. Inoue, A., Yanagisawa, M., Kimura, S., Kasuya, Y., Miyauchi, T., Goto, K., and Masaki, T. (1989) The human endothelin family: three structurally and pharmacologically distinct isopeptides predicted by three separate genes, *Proc. Natl. Acad. Sci. U.S.A. 86*, 2863−2867.
4. Masaki, T., Vane, J. R., and Vanhoutte, P. M. (1994) International Union of Pharmacology nomenclature of endothelin receptors, *Pharmacol. Rev. 46*, 137−142.
5. Sakurai, T., Yanagisawa, M., and Masaki, T. (1992) Molecular characterization of endothelin receptors, *Trends Pharmacol. Sci. 13*, 103−108.
6. Shetty, S. S., Okada, T., Webb, R. L., DelGrande, D., and Lappe, R. W. (1993) Functionally distinct endothelin B receptors in vascular endothelium and smooth muscle, *Biochem. Biophys. Res. Commun. 191*, 459−464.
7. Masaki, T. (2004) Historical review: endothelin, *Trends Pharmacol. Sci. 25*, 219−224.
8. Touyz, R. M., and Schiffrin, E. L. (2003) Role of endothelin in human hypertension, *Can. J. Physiol. Pharmacol. 81*, 533−541.
9. Orth, S. R., Viedt, C., Amann, K., and Ritz, E. (2001) Endothelin in renal diseases and cardiovascular remodeling in renal failure, *Intern. Med. 40*, 285−291.
10. Schmitz-Spanke, S., and Schipke, J. D. (2000) Potential role of endothelin-1 and endothelin antagonists in cardiovascular diseases, *Basic Res. Cardiol. 95*, 290−298.
11. Masaki, T., Ninomiya, H., Sakamoto, A., and Okamoto, Y., (1999) Structural basis of the function of endothelin receptor, *Mol. Cell. Biochem. 190*, 153−156.
12. Breu, V., Hashido, K., Broger, C., Miyamoto, C., Furuichi, Y., Hayes, A., Kalina, B., Loffler, B. M., Ramuz, H., and Clozel, M. (1995) Separable binding sites for the natural agonist endothelin-1 and the non-peptide antagonist bosentan on human endothelin-A receptors, *Eur. J. Biochem. 231*, 266−270.
13. Krystek, S. R., Jr., Patel, P. S., Rose, P. M., Fisher, S. M., Kienzle, B. K., Lach, D. A., Liu, E. C., Lynch, J. S., Novotny, J., and Webb, M. L. (1994) Mutation of peptide binding site in transmembrane region of a G protein-coupled receptor accounts for endothelin receptor subtype selectivity, *J. Biol. Chem. 17*, 12383−12386.
14. Lee, J. A., Elliott, J. D., Sutiphong, J. A., Friesen, W. J., Ohlstein, E. H., Stadel, J. M., Gleason, J. G., and Peishoff, C. E. (1994) Tyr-129 is important to the peptide ligand affinity and selectivity of human endothelin type A receptor, *Proc. Natl. Acad. Sci. U.S.A. 91*, 7164−7168.
15. Adachi, M., Furuichi, Y., and Miyamoto, C. (1994) Identification of a ligand-binding site of the human endothelin-A receptor and specific regions required for ligand selectivity, *Eur. J. Biochem. 220*, 37−43.

16. Zhu, G., Wu, L. H., Mauzy, C., Egloff, A. M., Mirzadegan, T., and Chung, F. Z. (1992) Replacement of lysine-181 by aspartic acid in the third transmembrane region of endothelin type B receptor reduces its affinity to endothelin peptides and sarafotoxin 6c without affecting G protein coupling, *J. Cell. Biochem. 50*, 159−164.
17. Sakamoto, A., Yanagisawa, M., Sawamura, T., Enoki, T., Ohtani, T., Sakurai, T., Nakao, K., Toyo-oka, T., and Masaki, T. (1993) Distinct subdomains of human endothelin receptors determine their selectivity to endothelin A-selective antagonist and endothelin B-selective agonists, *J. Biol. Chem. 268*, 8547−8553.
18. Adachi, M., Yang, Y. Y., Trzeciak, A., Furuichi, Y., and Miyamoto, C. (1992) Identification of a domain of ET_A receptor required for ligand binding, *FEBS Lett. 2*, 179−183.
19. Kauer, J. C., Erickson-Viitanen, S., Wolfe, H. R., Jr., and DeGrado, W. F. (1986) *p*-Benzoyl-L-phenylalanine, a new photoreactive amino acid. Photolabeling of calmodulin with a synthetic calmodulin-binding peptide, *J. Biol. Chem. 261*, 10695−10700.
20. Bremer, A. A., Leeman, S. E., and Boyd, N. D. (2001) Evidence for spatial proximity of two distinct receptor regions in the substance P (SP) neurokinin-1 receptor (NK-1R) complex obtained by photolabeling the NK-1R with *p*-benzoylphenylalanine3-SP, *J. Biol. Chem. 276*, 22857−22861.
21. Pérodin, J., Deraet, M., Auger-Messier, M., Boucard, A. A., Rihakova, L., Beaulieu, M.-E., Lavigne, P., Parent, J.-L., Guillemette, G., Leduc, R., and Escher, E. (2002) Residues 293 and 294 are ligand contact points of the human angiotensin type 1 receptor, *Biochemistry 41*, 14348−14356.
22. Boucard, A. A., Sauvé, S. S., Guillemette, G., Escher, E., and Leduc, R. (2003) Photolabelling the rat urotensin II/GPR14 receptor identifies a ligand-binding site in the fourth transmembrane domain, *Biochem. J. 370*, 829−838.
23. Kitada, C., Ohtaki, T., Masuda, Y., Masuo, Y., Nomura, H., Asami, T., Matsumoto, Y., Satou, M., and Fujino, M. (1993) Design and synthesis of ET_A receptor antagonists and study of ET_A receptor distribution, *J. Cardiovasc. Pharmacol. 22*, S128−131.
24. Pullen, M., Brown, G., and Nambi, P. (1997) Binding characteristics of [^{125}I]TTA-386, ETA-selective antagonist, *Neuropeptides 31*, 345−349.
25. Bunin, B. (1998) Combinatorial solid-phase synthesis, in *The Combinatorial Index*, pp 77−212, Academic Press, San Diego, CA.
26. Watakabe, T., Urade, Y., Takai, M., Umemura, I., and Okada, T. (1992) A reversible radioligand specific for the ET_B receptor, *Biochem. Biophys. Res. Commun. 185*, 867−873.
27. Boucard, A. A., Wilkes, B. C., Laporte, S. A., Escher, E., Guillemette, G., and Leduc, R. (2000) Photolabeling identifies position 172 of the human AT1 receptor as a ligand contact point: receptor-bound angiotensin II adopts an extended structure, *Biochemistry 39*, 9662−9670.
28. Boivin, S., Tessier, S., Aubin, J., Lampron, P., Detheux, M., and Fournier, A. (2004) Identification of a binding domain of the endothelin-B receptor using a selective IRL-1620-derived photoprobe, *Biochemistry 43*, 11516−11525.

BI0500933